Sudden increase in tidal response linked to calving and acceleration at a large Greenland outlet glacier

Julia de Juan,[1] Pedro Elósegui,[1] Meredith Nettles,[2] Tine B. Larsen,[3] James L. Davis,[4] Gordon S. Hamilton,[5] Leigh A. Stearns,[6] Morten L. Andersen,[3,7] Göran Ekström,[2] Andreas P. Ahlstrøm,[3] Lars Stenseng,[8] S. Abbas Khan,[8] and René Forsberg[8]

Received 19 March 2010; revised 7 May 2010; accepted 13 May 2010; published 23 June 2010.

[1] Large calving events at Greenland's largest outlet glaciers are associated with glacial earthquakes and near-instantaneous increases in glacier flow speed. At some glaciers and ice streams, flow is also modulated in a regular way by ocean tidal forcing at the terminus. At Helheim Glacier, analysis of geodetic data shows decimeter-level periodic position variations in response to tidal forcing. However, we also observe transient increases of more than 100% in the glacier's responsiveness to such tidal forcing following glacial-earthquake calving events. The timing and amplitude of the changes correlate strongly with the step-like increases in glacier speed and longitudinal strain rate associated with glacial earthquakes. The enhanced response to the ocean tides may be explained by a temporary disruption of the subglacial drainage system and a concomitant reduction of the friction at the ice-bedrock interface, and suggests a new means by which geodetic data may be used to infer glacier properties. **Citation:** de Juan, J., et al. (2010), Sudden increase in tidal response linked to calving and acceleration at a large Greenland outlet glacier, *Geophys. Res. Lett.*, *37*, L12501, doi:10.1029/2010GL043289.

1. Introduction

[2] Mass loss from the Greenland Ice Sheet is accelerating [*Velicogna*, 2009], partly due to dynamic changes at its outlet glaciers, which have exhibited increased flow speeds, terminus retreat, and thinning [e.g., *Joughin et al.*, 2004; *Krabill et al.*, 2004; *Howat et al.*, 2005; *Rignot and Kanagaratnam*, 2006; *Luckman et al.*, 2006; *Stearns and Hamilton*, 2007]. Observations and modeling suggest that these changes begin at the calving terminus and propagate upglacier [*Howat et al.*, 2005; *Stearns and Hamilton*, 2007; *Amundson et al.*, 2008; *Nettles et al.*, 2008; *Nick et al.*, 2009].

[3] Dynamic changes related to calving processes at these glaciers can occur on very short time scales, from minutes to hours [*Nettles et al.*, 2008; *Amundson et al.*, 2008]. Analysis of geodetic data from Helheim Glacier demonstrates that calving, glacial earthquakes, and rapid acceleration of the glacier trunk occur nearly simultaneously [*Nettles et al.*, 2008]. Current interpretations suggest that large icebergs produced in calving events overturn, exerting a force on the glacier and solid earth, causing glacial earthquakes [*Joughin et al.*, 2008a; *Nettles et al.*, 2008; *Amundson et al.*, 2008; *Tsai et al.*, 2008]. The resulting loss of mass at the calving front reduces resistive stresses near the terminus, and allows the glacier to accelerate [*Howat et al.*, 2005; *Nettles et al.*, 2008]. A similar acceleration of ice streams in Antarctica has been observed following loss of ice-shelf buttressing [*Scambos et al.*, 2004; *Rignot et al.*, 2004].

[4] In Antarctica, smaller forcings due to ocean tides have been observed to affect the dynamics of some ice streams, even far upglacier from the grounding line. Small earthquakes and stick-slip glacier flow at Whillans Ice Stream are controlled by diurnal tides [*Bindschadler et al.*, 2003; *Wiens et al.*, 2008], and Rutford Ice Stream responds at semi-diurnal, diurnal, semi-monthly, and semi-annual periods to tidal forcing [*Gudmundsson*, 2006; *Murray et al.*, 2007]. Most observations show that glaciers and ice streams flow faster during the falling tide and slower with the rising tide [*Anandakrishnan et al.*, 2003; *Gudmundsson*, 2006; *Murray et al.*, 2007], owing to the change in back pressure at the grounding line [*Anandakrishnan and Alley*, 1997; *Thomas*, 2007].

[5] Fast-flowing glaciers in Alaska have also shown speed variations related to ocean tides [e.g., *Meier and Post*, 1987], but little is known about tidal effects on the flow of outlet glaciers in Greenland. Previous workers observed tidal modulation of flow speed on a floating section of Kangerdlugssuaq Glacier [*Hamilton et al.*, 2006; *Davis et al.*, 2007], and the lower part of Jakobshavn Isbrae [*Echelmeyer et al.*, 1991], but characterization of the glacier response has been limited by sparse data. Here, we use a large dataset of geodetic observations to characterize rapid changes in outlet-glacier response to tidal forcing associated with calving events and glacial earthquakes.

2. Data and Methods

[6] During the boreal summer seasons of 2007 and 2008, we acquired continuous Global Positioning System (GPS) measurements at sampling intervals of 1–5 s at several

[1]Institute for Space Sciences, CSIC-IEEC, Barcelona, Spain.
[2]Lamont-Doherty Earth Observatory, Columbia University, Palisades, New York, USA.
[3]Geological Survey of Denmark and Greenland, Copenhagen, Denmark.
[4]Harvard-Smithsonian Center for Astrophysics, Cambridge, Massachusetts, USA.
[5]Climate Change Institute, University of Maine, Orono, Maine, USA.
[6]Department of Geology, University of Kansas, Lawrence, Kansas, USA.
[7]Center for Ice and Climate, Niels Bohr Institute, University of Copenhagen, Copenhagen, Denmark.
[8]DTU Space, National Space Institute, Copenhagen, Denmark.

0094-8276/10/2010GL043289

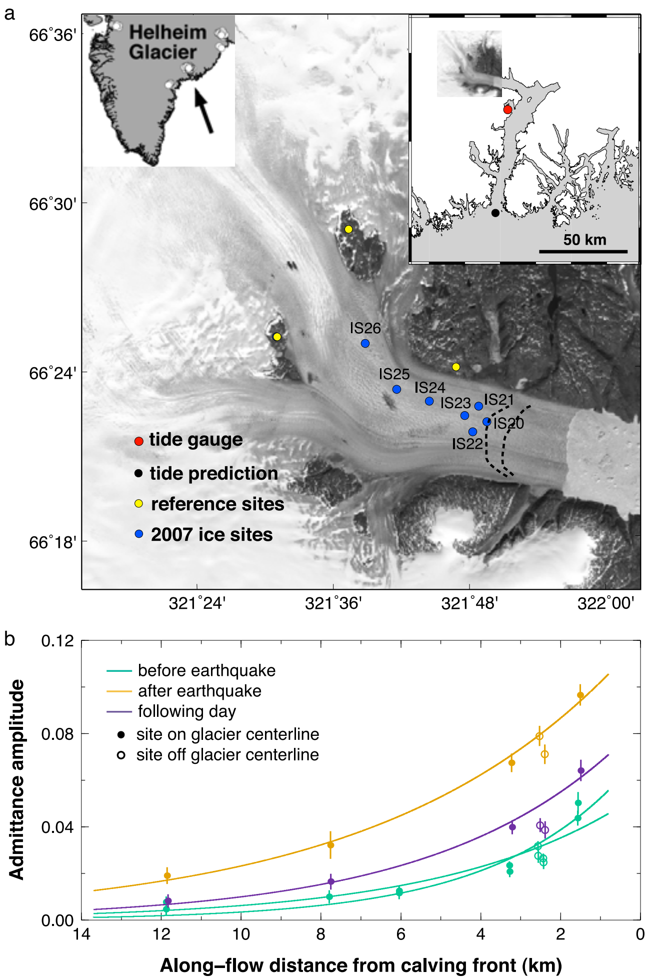

Figure 1. (a) Left inset: southern Greenland, white dots show the locations of glacial earthquakes [*Tsai and Ekström*, 2007]. Arrow marks the location of Helheim Glacier. Right inset: Map of the region showing the glacial fjord. Red dot: location of water-pressure tide gauge. Black dot: location for ocean-tide prediction. Main figure: Deployment location of GPS stations at Helheim Glacier in the summer of 2007, overlain on a 2001 LANDSAT image. Blue dots: ice stations used in the analysis of the events on days 189–190. Yellow dots: reference stations. Black dotted lines show the position of the calving front at two times during the summer (easternmost line, July 4; westernmost line, August 15). (b) Admittance of along-flow response to ocean-tidal forcing as a function of distance from the calving front position on day 185 (2007), fitted with an exponential function, for four days encompassing the time of the glacial earthquakes on days 189 and 190. The sites located off the glacier centerline are not included in the exponential fit.

locations on Helheim Glacier (Figure 1a), and at three nearby locations on bedrock, for a period of ~2 months [*Nettles et al.*, 2008]. We estimate the time-dependent position of the GPS sites on the surface of the glacier relative to the static antennas on bedrock at 15-s intervals using the TRACK software package [*Chen*, 1998], as described by *Nettles et al.* [2008].

[7] During part of the observing period, we also operated a water-pressure gauge ~35 km from the glacier terminus to obtain a record of ocean tides. To extend the tide record to the full GPS observing period, we use the AOTIM-5 model [*Padman and Erofeeva*, 2004] to compute the ocean-tide height at an open-ocean location near the mouth of the glacial fjord (Figure 1a). The predicted tide agrees well with observed water heights during periods when measurements are available. The measured tide in the fjord is in phase (within 3 minutes) with the predicted tide, and their amplitudes agree at the cm-level.

[8] We estimate the response of the glacier to the ocean tide by performing a least-squares fit to the geodetic position estimates using a model that includes a mean glacier flow velocity, a mean acceleration when warranted, and an admittance parameter relating the ocean tide height to deviations in glacier displacement from the mean flow. The admittance parameter is thus the ratio between the amplitude of the tidal response of the glacier and the amplitude of the ocean tide. We also estimate a delay between the ocean tide and the response of the glacier by performing a χ^2 grid search at 5-minute time steps. We compare the fits achieved using a constant-speed and a constant-acceleration model with an F-test at 95% confidence, and we also evaluate a constant-speed model that does not include a tidal signal, enabling us to assess the significance of the tidal signal and the acceleration for a given day and site. We analyze each day independently, and also perform fits to shorter time periods bounded by glacial earthquakes [*Nettles et al.*, 2008]. We consider data from ice sites located up to ~12 km behind the calving front (Figure 1a), where the amplitude of the tidal variations decays to ~1 cm.

3. Results

[9] During summer 2007, Helheim Glacier flowed at a mean speed of ~25 m/day near the calving front, and at ~12 m/day at locations ~25 km upglacier, as reported by *Nettles et al.* [2008]. In summer 2008, glacier flow was slower (the site located closest to the calving front flowed at a mean speed of ~20 m/day) and less variable. The largest variations in flow speed — step-like increases in glacier velocity that are coherent throughout the GPS network — are associated with glacial earthquakes [*Nettles et al.*, 2008]. These changes in flow velocity decrease with distance upglacier, resulting in an increase in longitudinal strain rate.

[10] The along-flow motion of Helheim Glacier varies such that the glacier position is advanced at low tide and retarded at high tide (Figure 2) with respect to mean flow. We interpret this out-of-phase response of the glacier to tidal forcing as resulting from stress fluctuations on the terminus caused by variations in hydrostatic pressure associated with the ocean tides [e.g., *Anandakrishnan and Alley*, 1997]. We observe variations in the time delay of the response of 0–4 hrs, but the accuracy of the time-delay estimates does not allow the identification of any propagation of the tidal signal along the glacier. For all days studied, the tidal admittance parameters show an exponential decay with distance from the calving front, consistent with observations and model results of previous workers [*Anandakrishnan and Alley*, 1997]. Results from several representative days are shown in Figure 1b. During the time periods considered here, we observe no significant tidal

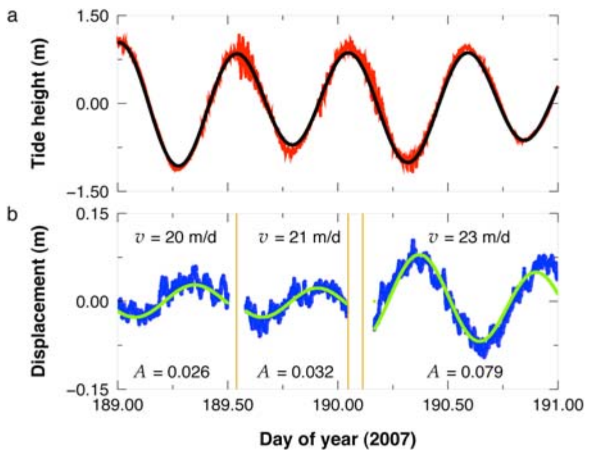

Figure 2. (a) Black line shows predicted ocean tide at an ocean location near the mouth of the glacial fjord (Figure 1a). Red line shows observed tide within the fjord. (b) Blue dots show estimates of horizontal position (site IS22) along the direction of glacier flow relative to a best-fit mean speed v, for three time periods separated by glacial earthquakes. Green line shows tidal function fitted to these estimates, with admittances A. The rms misfit is less than 16 mm for the examples shown, and is typical for our analyses. Yellow lines indicate the times of glacial earthquakes [*Nettles et al.*, 2008].

signal in the vertical or cross-flow directions, indicating that the glacier tongue was grounded at the times and locations (very near the calving front) that we examine.

[11] Typically, tidal admittance amplitudes vary little from day to day. However, following glacial earthquakes the tidal admittance increases suddenly by a factor of as much as ~2.5 (Figure 2). During the two seasons, six large glacial earthquakes occurred [*Nettles et al.*, 2008], clustered in three different time periods: two in summer 2007 and one in summer 2008. The example shown here (Figures 1–3a), from 2007 and encompassing three earthquakes, is associated with the largest increase in velocity and largest increase in tidal response. The other events, occurring for different positions of the calving front in the fjord, show consistent behavior (Figure 3b).

[12] An immediate increase in tidal response following the earthquakes is clear from visual inspection of the signal in Figure 2b. Following the two glacial earthquakes on day 190, the admittance of the tidal signal increased by a factor of ~2.5, coincident with an increase in velocity of ~2 m/d. The first of the earthquakes shown in Figure 2b, on day 189, is associated with smaller changes in tidal response and flow speed. Like the change in flow velocity [*Nettles et al.*, 2008], the change in tidal admittance decreases with distance upglacier (Figure 1).

[13] The enhanced tidal response lasts for one to two days after the glacial earthquake. The decrease in tidal response is temporally linked to a deceleration of the glacier (Figure 3a). However, unlike the tidal response, the glacier velocity typically recovers only partially. Both the magnitude of the change in tidal response following a glacial earthquake and its subsequent decrease correlate with changes in flow speed observed at those times (Figure 3b). Other variations in tidal response during the summer are small compared with changes associated with glacial earthquakes. As expected, the ocean-tide record varies smoothly and continuously throughout the period of increased tidal response (Figure 2a), with the exception of small tsunamis caused by the calving process [*Nettles et al.*, 2008] that attenuate well before the tidal response recovers.

4. Discussion and Conclusions

[14] Our results indicate a temporal relationship between the glacier's enhanced response to tidal forcing and the flow

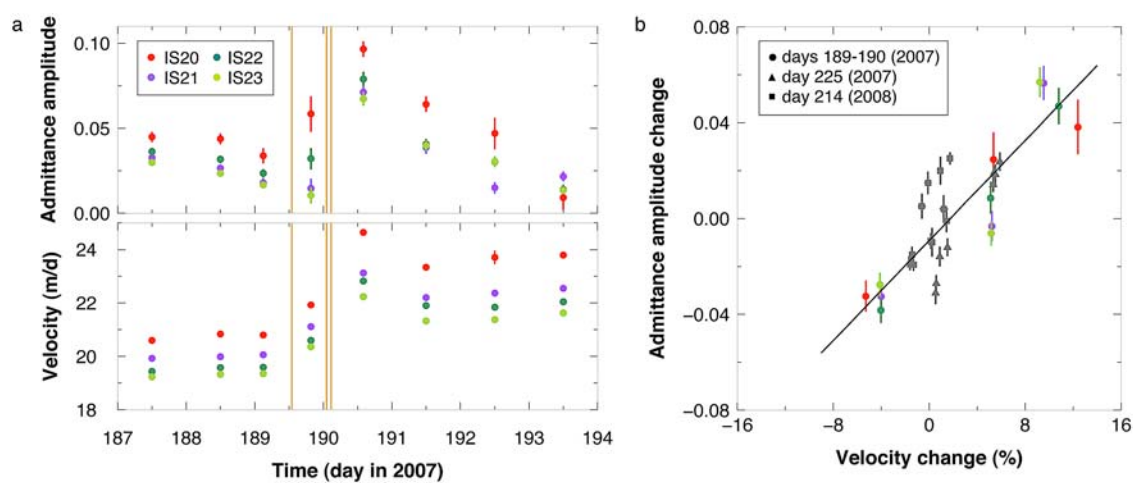

Figure 3. (a) Admittance amplitudes for the glacier response to the ocean tide in the along-flow component of motion, and velocity of the four GPS stations located closest to the calving front (see Figure 1a) for seven days in 2007 encompassing the time of three glacial earthquakes (yellow lines). Uncertainties are plotted as vertical bars. (b) Correlation between admittance-amplitude change and fractional velocity change for the four sites located closest to the calving front, with best linear fit (black line; correlation coefficient of 0.86). Values are plotted for each of the two days following the glacial earthquakes on days 189 and 190, 2007 (color coded as in Figure 3a), day 225, 2007, and day 214, 2008. Uncertainties are plotted as horizontal and vertical bars. For many estimates, error bars are smaller than the size of the symbols.

acceleration and increased longitudinal strain rates that follow glacial-earthquake calving. Although the tidal stress is applied at the glacier terminus, the change in sensitivity to tidal forcing is observed at least 12 km upglacier after a glacial-earthquake calving event, indicating a coupling of flow characteristics over at least this distance. The loss of ice itself is unlikely to be the cause of the increased tidal response: while sustained flow-speed increases can be attributed to a long-term loss of ice at the glacier terminus, the rapid recovery of admittance amplitudes to pre-event values demonstrates that the change in distance to the calving front is not the primary control on the temporal variation in glacier tidal response. The recovery also occurs before the glacier front has readvanced significantly in the fjord, since the rate of advance is limited by the speed of glacier flow. A temporary decrease in resistance at the glacier bed would, however, enable the glacier to respond with higher amplitude to the tides.

[15] Although the velocity of fast-flowing outlet glaciers is less sensitive than that of ice sheets to enhanced meltwater input [*Joughin et al.*, 2008b; *van de Wal et al.*, 2008] it has been shown that they can respond to fluctuations in melt [*Joughin et al.*, 2008b; *Andersen et al.*, 2009]. At Helheim Glacier, velocity variations of up to ~5% have been found to be correlated with melt fluctuations with a 1-day time lag, the correlation being more significant near the front of the glacier [*Andersen et al.*, 2009].

[16] Following large calving events associated with glacial earthquakes, the glacier experiences an increase in surface velocity and strain rate. Since fast-moving outlet glaciers flow mainly by basal sliding, we expect a change in strain rate at the glacier surface to lead to a similar change at the glacier base. This change in strain rate may disrupt the subglacial hydrologic system, reducing the volume of water that can be accommodated in subglacial channels and increasing basal water pressure, further lubricating the ice-bedrock interface and enabling the glacier to enhance its response to the tides. Such reorganization of the basal hydrological system has been shown to act as a mechanism for glacier surges [e.g., *Kamb et al.*, 1985].

[17] At Helheim, the disruption of the hydrological system is expected to be temporary, with more efficient drainage re-established as strain rate is reduced. Furthermore, this effect would cause a temporary additional acceleration, above the longer-term speedup caused by the loss of resisting forces at the terminus, that would recover at the same time as the tidal response.

[18] Alternatively, the nonlinear rheology of the ice may provide a mechanism for enhanced response to tidal forcing as velocity and strain rate increase.

[19] Our analysis demonstrates that large calving events rapidly change the response of Greenland's outlet glaciers to steady forcings, such as the ocean tide, in addition to inducing both temporary and persistent changes in the glaciers' flow regime, and highlights the need for understanding the mechanisms that induce such responses.

[20] **Acknowledgments.** This work was supported by the Spanish Ministry of Science and Innovation (MICINN), the Gary Comer Science and Education Foundation, the U.S. National Science Foundation, the Danish Commission for Scientific Research in Greenland (KVUG), the Geological Survey of Denmark and Greenland (GEUS), Geocenter Copenhagen, the Danish National Space Center, and NASA. JdJ acknowledges a CSIC pre-doctoral fellowship. GPS equipment and technical support were provided by UNAVCO, Inc. We thank S. Anandakrishnan and an anonymous reviewer, whose comments helped improve the manuscript.

References

Amundson, J. M., M. Truffer, M. P. Lüthi, M. Fahnestock, M. West, and R. J. Motyka (2008), Glacier, fjord, and seismic response to recent large calving events, Jakobshavn Isbræ, Greenland, *Geophys. Res. Lett.*, *35*, L22501, doi:10.1029/2008GL035281.

Anandakrishnan, S., and R. B. Alley (1997), Tidal forcing of basal seismicity of ice stream C, West Antarctica, observed far inland, *J. Geophys. Res.*, *102*, 15,183–15,196.

Anandakrishnan, S., D. E. Voigt, R. B. Alley, and M. A. King (2003), Ice stream D flow speed is strongly modulated by the tide beneath the Ross Ice Shelf, *Geophys. Res. Lett.*, *30*(7), 1361, doi:10.1029/2002GL016329.

Andersen, M. L., M. Nettles, T. Larsen, P. Elosegui, G. S. Hamilton, L. A. Stearns, D. van As, J. de Juan, and J. L. Davis (2009), Surface melt and its effect on Helheim Glacier dynamics, *Eos Trans. AGU*, *90*(52), Fall Meet. Suppl., Abstract C21D-0465.

Bindschadler, R. A., M. A. King, R. B. Alley, S. Anandakrishnan, and L. Padman (2003), Tidally controlled stick-slip discharge of a West Antarctic Ice Stream, *Science*, *301*, 1087–1089.

Chen, G. (1998), GPS kinematic positioning for the airborne laser altimetry at Long Valley, California, Ph.D. thesis, Mass. Inst. of Technol., Cambridge.

Davis, J. L., P. Elosegui, G. S. Hamilton, L. A. Stearns, M. Langer, M. Nettles, and T. B. Larsen (2007), Mechanisms for tidally induced glacier deformation and flow variations, east Greenland, *Eos Trans. AGU*, *88*(52), Fall Meet. Suppl., Abstract G33B-1234.

Echelmeyer, K., T. Clarke, and W. Harrison (1991), Surficial glaciology of Jakobshavns Isbræ, West Greenland: Part I. Surface morphology, *J. Glaciol.*, *37*, 368–382.

Gudmundsson, G. H. (2006), Fortnightly variations in the flow velocity of Rutford Ice Stream, West Antarctica, *Nature*, *444*, 1063–1064.

Hamilton, G. S., et al. (2006), Tidal modulation of ice flow on Kangerdlugssuaq and Helheim glaciers, east Greenland, from high-rate GPS measurements, *Eos Trans. AGU*, *87*(52), Fall Meet. Suppl., Abstract C51C-02.

Howat, I. M., I. Joughin, S. Tulaczyk, and S. Gogineni (2005), Rapid retreat and acceleration of Helheim Glacier, east Greenland, *Geophys. Res. Lett.*, *32*, L22502, doi:10.1029/2005GL024737.

Joughin, I., W. Abdalati, and M. Fahnestock (2004), Large fluctuations in speed on Greenland's Jakobshavn Isbræ Glacier, *Nature*, *432*, 608–610.

Joughin, I., I. Howat, R. B. Alley, G. Ekström, M. Fahnestock, T. Moon, M. Nettles, M. Truffer, and V. C. Tsai (2008a), Ice-front variation and tidewater behavior on Helheim and Kangerdlugssuaq glaciers, Greenland, *J. Geophys. Res.*, *113*, F01004, doi:10.1029/2007JF000837.

Joughin, I., S. B. Das, M. A. King, B. E. Smith, I. M. Howat, and T. Moon (2008b), Seasonal speedup along the western flank of the Greenland Ice Sheet, *Science*, *320*, 781–783.

Kamb, B., C. F. Raymond, W. D. Harrison, H. Engelhardt, K. A. Echelmeyer, N. Humphrey, M. M. Brugman, and T. Pfeffer (1985), Glacier surge mechanism: 1982–1983 surge of Variegated Glacier, Alaska, *Science*, *227*, 469–479.

Krabill, W., et al. (2004), Greenland Ice Sheet: Increased coastal thinning, *Geophys. Res. Lett.*, *31*, L24402, doi:10.1029/2004GL021533.

Luckman, A., T. Murray, R. de Lange, and E. Hanna (2006), Rapid and synchronous ice-dynamic changes in east Greenland, *Geophys. Res. Lett.*, *33*, L03503, doi:10.1029/2005GL025428.

Meier, M. F., and A. Post (1987), Fast tidewater glaciers, *J. Geophys. Res.*, *92*, 9051–9058.

Murray, T., A. M. Smith, M. A. King, and G. P. Weedon (2007), Ice flow modulated by tides at up to annual periods at Rutford Ice Stream, West Antarctica, *Geophys. Res. Lett.*, *34*, L18503, doi:10.1029/2007GL031207.

Nettles, M., et al. (2008), Step-wise changes in glacier flow speed coincide with calving and glacial earthquakes at Helheim Glacier, Greenland, *Geophys. Res. Lett.*, *35*, L24503, doi:10.1029/2008GL036127.

Nick, F. M., A. Vieli, I. M. Howat, and I. Joughin (2009), Large-scale changes in Greenland outlet glacier dynamics triggered at the terminus, *Nat. Geosci.*, *2*, 110–114.

Padman, L., and S. Erofeeva (2004), A barotropic inverse tidal model for the Arctic Ocean, *Geophys. Res. Lett.*, *31*, L02303, doi:10.1029/2003GL019003.

Rignot, E., and P. Kanagaratnam (2006), Changes in the velocity structure of the Greenland Ice Sheet, *Science*, *311*, 986–990.

Rignot, E., G. Casassa, P. Gogineni, W. Krabill, A. Rivera, and R. Thomas (2004), Accelerated ice discharge from the Antarctic Peninsula following the collapse of Larsen B Ice Shelf, *Geophys. Res. Lett.*, *31*, L18401, doi:10.1029/2004GL020697.

Scambos, T. A., J. A. Bohlander, C. A. Shuman, and P. Skvarca (2004), Glacier acceleration and thinning after ice shelf collapse in the Larsen B embayment, Antarctica, *Geophys. Res. Lett.*, *31*, L18402, doi:10.1029/2004GL020670.

Stearns, L. A., and G. S. Hamilton (2007), Rapid volume loss from two East Greenland outlet glaciers quantified using repeat stereo satellite imagery, *Geophys. Res. Lett.*, *34*, L05503, doi:10.1029/2006GL028982.

Thomas, R. H. (2007), Tide-induced perturbations of glacier velocities, *Global Planet. Change*, *59*, 217–224.

Tsai, V. C., and G. Ekström (2007), Analysis of glacial earthquakes, *J. Geophys. Res.*, *112*, F03S22, doi:10.1029/2006JF000596.

Tsai, V. C., J. R. Rice, and M. Fahnestock (2008), Possible mechanisms for glacial earthquakes, *J. Geophys. Res.*, *113*, F03014, doi:10.1029/2007JF000944.

van de Wal, R. S. W., W. Boot, M. R. van den Broeke, C. J. P. P. Smeets, C. H. Reijmer, J. J. A. Donker, and J. Oerlemans (2008), Large and rapid melt-induced velocity changes in the ablation zone of the Greenland Ice Sheet, *Science*, *321*, 111–113.

Velicogna, I. (2009), Increasing rates of ice mass loss from the Greenland and Antarctic ice sheets revealed by GRACE, *Geophys. Res. Lett.*, *36*, L19503, doi:10.1029/2009GL040222.

Wiens, D. A., S. Anandakrishnan, J. P. Winberry, and M. A. King (2008), Simultaneous teleseismic and geodetic observations of the stick-slip motion of an Antarctic Ice Stream, *Nature*, *453*, 770–775.

A. P. Ahlstrøm, M. L. Andersen, and T. B. Larsen, Geological Survey of Denmark and Greenland, Oester Voldgade 10, DK-1350 Copenhagen, Denmark.

J. L. Davis, Harvard-Smithsonian Center for Astrophysics, 60 Garden St., MS 42, Cambridge, MA 02138, USA.

J. de Juan and P. Elósegui, Institute for Space Sciences, CSIC-IEEC, E-Nexus 201, Gran Capita 2, E-08034 Barcelona, Spain. (dejuan@ice.csic.es)

G. Ekström and M. Nettles, Lamont-Doherty Earth Observatory, Columbia University, 61 Rte. 9W, Palisades, NY 10964, USA.

R. Forsberg, S. A. Khan, and L. Stenseng, DTU Space, National Space Institute, Juliane Maries Vej 30, DK-2100 Copenhagen, Denmark.

G. S. Hamilton, Climate Change Institute, University of Maine, 303 Bryand Global Sciences Bldg., Orono, ME 04469, USA.

L. A. Stearns, Department of Geology, University of Kansas, 1475 Jayhawk Blvd., Room 120, Lawrence, KS 66045, USA.